ECCOMAS Thematic Conference on Mechanical Response of Composites
P. P. Camanho et.al. (eds.)
Porto, Portugal, 12–14 September 2007

STUDIES ON DYNAMIC BEHAVIOR OF FUNCTIONALLY GRADED HOLLOW CYLINDERS

M. Tahani[1] **and T. Talebian**[2]

Department of Mechanical Engineering, Faculty of Engineering, Ferdowsi University of Mashhad,
P.O.Box 91775-1111, Mashhad, Iran
[1] e-mail: mtahani@ferdowsi.um.ac.ir

[2] e-mail: t_talebian@yahoo.com

Keywords: Functionally Graded Cylinder, FEM, Dynamic Response, Transient Waves.

Abstract. *This article presents the analysis of functionally graded hollow cylinders with finite length under axisymmetric dynamic loads. It is assumed that the functionally graded cylinder is comprised of metal-phase and ceramic-phase and material properties are graded in the thickness direction of the cylinder according to a power law distribution. The axisymmetric governing equations of motion are derived. To solve them, two dimensional finite element and Newmark's methods are used. By this method, loading in longitudinal and radial directions can be applied as an arbitrary function of time and coordinates. In a simple case, an internal pressure which increases exponentially from zero to a final value is applied. Radial displacement for long time is obtained and compared to analytical result of an isotropic thick hollow cylinder under uniform internal pressure. In another case, internal pressure is applied as a triangular pulse and dynamic response is investigated. By using the fast Fourier transform (FFT), the time response is transferred to frequency domain and natural frequencies are illustrated. As another axisymmetric load, a radial line load which is uniformly distributed along circumferential direction is considered and longitudinal wave propagation through the length of the cylinder is illustrated. Also the mean velocities of wave propagation are obtained. Numerical results for thick cylinders and cylindrical shells are obtained and compared with the results for isotropic cylinders.*

1 INTRODUCTION

A functionally graded material (FGM) is usually a combination of two material phases that has a gradual transition from one material at one surface to another one at the opposite surface. This transition allows the creation of multiple properties (or functions) without any mechanically weak junction or interface. Furthermore, the gradual change of properties can be tailored to different applications and service environments. It is possible with these materials to obtain a combination of properties that cannot be achieved in conventional monolithic materials. For example, thermal protection plate structures made of a two phase ceramic/metal functionally graded (FG) composite provide heat and corrosion resistance on the ceramic-rich surface while maintaining the structural strength and stiffness by the metal-rich surface. Moreover, FGMs allow for spatial optimization by grading the volume fractions of two or more constituents to improve the response of structures. If properly designed, FGMs can offer various advantages such as reduction of thermal stresses, minimization of stress concentration or intensity factors and attenuation of stress waves. Hence, FGMs have gained potential applications in a wide variety of engineering components or systems including the rocking motor casing, armor plating, heat-engine components, packaging encapsulates, thermoelectric generators, and human implants, just to name a few.

There are some works done in response of functionally graded cylinders under dynamic thermal and mechanical loads. Gong et al. [1] used Reddy's third order shear deformation theory (without incorporating transverse normal deformation) to present an analytical solution to predict the transient response of simply supported FGM cylindrical shells subjected to low-velocity impact by a solid striker. A solution for guided waves in graded cylinders making use of Nelson's numerical–analytical method [2] was first introduced in 2002 by Han et al. [3]. Then, they [4] have presented a numerical method for analyzing transient waves in FGM cylinders. In their method, the FGM shell is divided into layer elements with three nodal lines along the wall thickness. The material property within each element is assumed to vary linearly in the thickness direction. Also, Han et al. [5] employed Fourier transformation and modal analysis to propose a numerical method for analyzing transient waves in cylindrical shells of an FGM excited by impact point loads. Loy et al. [6] and Pradhan et al. [7] have investigated the vibration behavior of functionally graded cylindrical shells based on Love's theory and the Rayleigh–Ritz method. Their studies revealed that the frequency characteristics of functionally graded cylindrical shells are similar to those of isotropic shells. Yang and Shen [8] used Reddy's higher-order shear deformation shell theory to investigate free vibration and dynamic instability of functionally graded cylindrical panels subjected to thermo-mechanical loads consisting of a steady temperature change, static and periodically pulsating forces in axial direction. Also, Yang and Shen [9] developed a semi-analytical approach for dynamic buckling of an FGM cylindrical panel loaded by a combination of static and periodic axial forces and under a uniform temperature change. Sofiyev [10] studied the stability of cylindrical shells composed of functionally gradient material subjected to axial compressive load varying as a power function of time. Also, Sofiyev [11, 12] studied stability of functionally graded cylindrical and conical shells, respectively under a periodic time dependent external pressure. Elmaimouni et al. [13] made use of Legendre polynomials and harmonic functions to develop a numerical method for calculating guided wave propagation in an FGM infinite cylinder. Kadoli and Ganesan [14] presented linear (LN) thermal buckling and free vibration analysis for functionally graded cylindrical shells with clamped–clamped boundary condition based on temperature-dependent material properties. Shakeri et al. [15] have studied vibrations and radial wave propagation in FGM thick hollow cylinders with considering the FGM cylinder is made of many isotropic sub cylinders. Parametric resonance of simply supported

FGM cylindrical shells under periodic axial loading was studied by Ng et al. [16]. A second order differential equation with periodic coefficients of the Mathieu-Hill type is derived. The Bolotin's first approximation is used to evaluate the periodic solution. They report that the natural frequencies and dynamic instability regions can be fairly controlled by appropriately varying the power law exponent. Recently Ng et al. [17] developed an efficient finite element formulation based on the first order shear deformation theory for active control of FGM shells in the frequency domain. They also illustrated the application of their formulation for a cantilever FGM shell with piezoelectric sensor and actuator layers and subjected to a harmonic excitation. Natural frequencies can be controlled to desired values by adjusting the displacement control gain or the volume fraction of the constituent materials. Vibration amplitudes can be controlled by increasing the damping via displacement velocity feedback gain.

Fuchiyama and Noda [18] have developed a computer program to analyze the transient heat transfer and transient thermal stresses in FGM components by finite element method. Reddy and Chin [19] have developed a coupled as well as an uncoupled thermoelastic finite element formulation to analyze the thermomechanical behavior of functionally graded cylinders and plates subjected to abrupt thermal loading. Awaji and Sivakumar [20] analyzed numerically the steady-state and transient temperature distributions and related thermal stress distribution in the FGM cylinder composed of mullite-molybdenum system. Thermal stability of FGM circular cylindrical shells based on the Donnell stability equations are investigated by Eslami and Shahsiah [21]. Obata et al. [22] presented the solution for thermal stresses of a thick hollow cylinder made of FGM, under a two-dimensional transient temperature distribution.

In mentioned studies, multi-layered method has been used widely, in which FGM cylinder is divided into layer elements and material properties in each element are approximated to be constant or increasing linearly. In this work, distribution of material properties in the thickness direction is considered exactly according to a power low distribution. The governing equations of motion are solved by two dimensional finite element and Newmark's methods. By this method, we can apply loads in longitudinal and radial directions as an arbitrary function of time and coordinates.

2 THEORETICAL FORMULATION

2.1 Material properties definition for functionally graded shells

Here we consider an FGM cylinder, which is made of a mixture of ceramic and metal. The outer surface of the cylinder is metal-rich whereas the inner surface is ceramic-rich and material properties are graded in the thickness direction of the cylinder according to a power law distribution which is:

$$V = \left(V_{out} - V_{in}\right)\left(\frac{r - r_{in}}{r_{out} - r_{in}}\right)^{n} + V_{in} \tag{1}$$

where V_{in} and V_{out} are material properties in the inner and outer surfaces of the cylinder and volume fraction exponent n represents the material variation profile through the cylinder thickness, which is always equal or greater than zero, and may be varied to obtain the optimum distribution of the constituent materials. The value $n = 0$ represents a fully metal and infinity represents a fully ceramic cylinder.

2.2 Equations of motion

Consider a functionally graded cylinder with finite length subjected to axisymmetric loads. Since the geometry of the cylinder and the load are independent of circumferential direction, the problem is axisymmetric. The governing equations of motion for this case are:

$$\begin{aligned}\frac{\partial \sigma_r}{\partial r}+\frac{\sigma_r-\sigma_\theta}{r}+\frac{\partial \sigma_{rz}}{\partial z}&=\rho\frac{\partial^2 u_r}{\partial t^2}\\ \frac{\partial \sigma_{rz}}{\partial r}+\frac{\partial \sigma_z}{\partial z}+\frac{1}{r}\sigma_{rz}&=\rho\frac{\partial^2 u_z}{\partial t^2}\end{aligned} \tag{2}$$

Also, the strain-deflection relations in cylindrical coordinates are:

$$\begin{aligned}\varepsilon_r&=\frac{\partial u_r}{\partial r},\quad \varepsilon_\theta=\frac{u_r}{r},\quad \varepsilon_z=\frac{\partial u_z}{\partial z}\\ \gamma_{r\theta}&=\frac{\partial u_\theta}{\partial r}-\frac{u_\theta}{r},\quad \gamma_{rz}=\frac{\partial u_z}{\partial r}+\frac{\partial u_r}{\partial z},\quad \gamma_{\theta z}=\frac{\partial u_\theta}{\partial z}\end{aligned} \tag{3}$$

The linear constitutive relations are:

$$\begin{aligned}\begin{Bmatrix}\sigma_z\\ \sigma_\theta\\ \sigma_r\end{Bmatrix}&=\begin{bmatrix}C_{11}&C_{12}&C_{12}\\ C_{12}&C_{11}&C_{12}\\ C_{12}&C_{12}&C_{11}\end{bmatrix}\left(\begin{Bmatrix}\varepsilon_z\\ \varepsilon_\theta\\ \varepsilon_r\end{Bmatrix}-\begin{Bmatrix}\alpha\\ \alpha\\ \alpha\end{Bmatrix}\Delta T\right)\\ \sigma_{r\theta}&=C_{66}\gamma_{r\theta},\quad \sigma_{rz}=C_{66}\gamma_{rz},\quad \sigma_{z\theta}=C_{66}\gamma_{z\theta}\end{aligned} \tag{4}$$

where components of stiffness matrix are:

$$C_{11}=\frac{E(1-\nu)}{(1+\nu)(1-2\nu)},\quad C_{12}=\frac{E\nu}{(1+\nu)(1-2\nu)},\quad C_{66}=(C_{11}-C_{12})/2 \tag{5}$$

Substituting Eqs. (3) into (4) gives stress deflection relations as follows:

$$\begin{aligned}\sigma_z&=C_{11}\frac{\partial u_z}{\partial z}+C_{12}\left(\frac{u_r}{r}+\frac{\partial u_r}{\partial r}\right)\\ \sigma_\theta&=C_{11}\frac{u_r}{r}+C_{12}\left(\frac{\partial u_z}{\partial z}+\frac{\partial u_r}{\partial r}\right)\\ \sigma_r&=C_{11}\frac{\partial u_r}{\partial r}+C_{12}\left(\frac{u_r}{r}+\frac{\partial u_z}{\partial z}\right)\\ \sigma_{rz}&=C_{66}\left(\frac{\partial u_z}{\partial r}+\frac{\partial u_r}{\partial z}\right)\end{aligned} \tag{6}$$

Also by substituting Eqs. (6) into (2), two coupled partial differential equations are obtained as:

$$\frac{\partial}{\partial r}\left(C_{66}\left(\frac{\partial u_z}{\partial r}+\frac{\partial u_r}{\partial z}\right)\right)+\frac{C_{66}}{r}\left(\frac{\partial u_z}{\partial r}+\frac{\partial u_r}{\partial z}\right)+\frac{\partial}{\partial z}\left(C_{11}\frac{\partial u_z}{\partial z}+C_{12}\left(\frac{u_r}{r}+\frac{\partial u_r}{\partial r}\right)\right)=\rho\frac{\partial^2 u_z}{\partial t^2}$$

$$\frac{\partial}{\partial r}\left(C_{11}\frac{\partial u_r}{\partial r}+C_{12}\left(\frac{u_r}{r}+\frac{\partial u_z}{\partial z}\right)\right)+\frac{C_{12}-C_{11}}{r}\left(\frac{u_r}{r}-\frac{\partial u_r}{\partial r}\right)+\frac{\partial}{\partial z}\left(C_{66}\left(\frac{\partial u_z}{\partial r}+\frac{\partial u_r}{\partial z}\right)\right)=\rho\frac{\partial^2 u_r}{\partial t^2} \tag{7}$$

which are known as Navier's equations.

3 FINITE ELEMENT SOLUTION

3.1 Weak forms

In order to solve the Navior equations in (7), first we obtain weak forms as:

$$\begin{aligned}&\int\left\{\frac{\partial w_1}{\partial r}\left(C_{11}\frac{\partial u_r}{\partial r}+C_{12}\left(\frac{u_r}{r}+\frac{\partial u_z}{\partial z}\right)\right)+\frac{\partial w_1}{\partial z}\left(C_{66}\left(\frac{\partial u_z}{\partial r}+\frac{\partial u_r}{\partial z}\right)\right)\right.\\&\left.-w_1\frac{C_{12}-C_{11}}{r}\left(\frac{u_r}{r}-\frac{\partial u_r}{\partial r}\right)+\rho w_1\ddot{u}_r\right\}rdrdz-\oint w_1 t_r\,ds=0\\&\int\left\{\frac{\partial w_2}{\partial r}\left(C_{66}\left(\frac{\partial u_z}{\partial r}+\frac{\partial u_r}{\partial z}\right)\right)+\frac{\partial w_2}{\partial z}\left(C_{11}\frac{\partial u_z}{\partial z}+C_{12}\left(\frac{u_r}{r}+\frac{\partial u_r}{\partial r}\right)\right)\right.\\&\left.-w_2\frac{C_{66}}{r}\left(\frac{\partial u_z}{\partial r}+\frac{\partial u_r}{\partial z}\right)+\rho w_1\ddot{u}_z\right\}rdrdz-\oint w_2 t_z\,ds=0\end{aligned} \tag{8}$$

where w_1 and w_2 are weight functions and t_r and t_z are force tractions in boundary conditions as:

$$\begin{aligned}t_r&=\sigma_r n_r+\sigma_{rz}n_z\\t_z&=\sigma_z n_z+\sigma_{rz}n_r\end{aligned} \tag{9}$$

3.2 Finite element modelling

Here rectangular elements with two degrees of freedom in each node are used to model the two dimensional problem. The axisymmetric elements are considered in a cross-section of the cylinder, as shown in Figure 1.

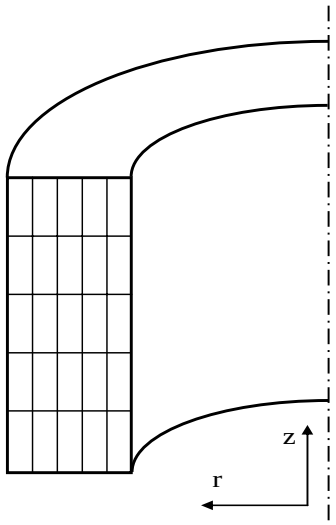

Figure 1: Arrangement of elements in the cylinder.

Also, linear interpolation functions are selected as:

$$\psi_1=\left(1-\frac{r}{a}\right)\left(1-\frac{z}{b}\right),\quad \psi_2=\frac{r}{a}\left(1-\frac{z}{b}\right),\quad \psi_3=\frac{z}{b}\left(1-\frac{r}{a}\right),\quad \psi_4=\frac{z}{b}.\frac{r}{a} \tag{10}$$

Displacements are approximated as follows:

$$u_r=\sum_{j=1}^{n_c}u_j\psi_j,\quad u_z=\sum_{j=1}^{n_c}v_j\psi_j \tag{11}$$

Weight function can also be replaced by interpolation functions. Therefore, weak forms are obtained as the following:

$$\begin{aligned}
&\int\left\{C_{11}\frac{\partial\psi_i}{\partial r}\frac{\partial\psi_j}{\partial r}u_j+C_{12}\frac{\partial\psi_i}{\partial r}\frac{\psi_j}{r}u_j+C_{12}\frac{\partial\psi_i}{\partial r}\frac{\psi_j}{\partial z}v_j+C_{66}\frac{\partial\psi_i}{\partial z}\frac{\partial\psi_j}{\partial r}v_j+C_{66}\frac{\partial\psi_i}{\partial z}\frac{\psi_j}{\partial z}u_j\right.\\
&\left.-\frac{C_{12}-C_{11}}{r}\frac{\psi_i}{r}\psi_j u_j+\frac{C_{12}-C_{11}}{r}\frac{\partial\psi_j}{\partial r}\psi_i u_j+\rho\psi_i\psi_j\ddot{u}_j\right\}rdrdz=\oint\psi_i t_r\\
&\int\left\{C_{66}\frac{\partial\psi_i}{\partial r}\frac{\partial\psi_j}{\partial r}v_j+C_{66}\frac{\partial\psi_i}{\partial r}\frac{\partial\psi_j}{\partial z}u_j+C_{11}\frac{\partial\psi_i}{\partial z}\frac{\psi_j}{\partial z}v_j+C_{12}\frac{\partial\psi_i}{\partial z}\frac{\psi_j}{r}u_j+C_{12}\frac{\partial\psi_i}{\partial z}\frac{\psi_j}{\partial r}u_j\right.\\
&\left.-\frac{C_{66}}{r}\frac{\partial\psi_j}{\partial r}\psi_i v_j-\frac{C_{66}}{r}\frac{\partial\psi_j}{\partial z}\psi_i u_j+\rho\psi_i\psi_j\ddot{v}_j\right\}rdrdz=\oint\psi_i t_z\,ds
\end{aligned} \tag{12}$$

Eqs. (12) can be written in the matrix form as:

$$\begin{bmatrix}M&0\\0&M\end{bmatrix}\begin{Bmatrix}\ddot{u}\\\ddot{v}\end{Bmatrix}+\begin{bmatrix}k_{11}&k_{12}\\k_{21}&k_{22}\end{bmatrix}\begin{Bmatrix}u\\v\end{Bmatrix}=\begin{Bmatrix}F_1\\F_2\end{Bmatrix} \tag{13}$$

where

$$\begin{aligned}
M&=\int\rho\psi_i\psi_j\,rdrdz\\
k_{11}&=\int\left\{C_{11}\frac{\partial\psi_i}{\partial r}\frac{\partial\psi_j}{\partial r}+C_{12}\frac{\partial\psi_i}{\partial r}\frac{\psi_j}{r}-\frac{C_{12}-C_{11}}{r}\frac{\psi_i}{r}\psi_j\right.\\
&\left.+\frac{C_{12}-C_{11}}{r}\frac{\partial\psi_j}{\partial r}\psi_i+C_{66}\frac{\partial\psi_i}{\partial z}\frac{\partial\psi_j}{\partial z}\right\}rdrdz\\
k_{12}&=\int\left\{C_{12}\frac{\partial\psi_i}{\partial r}\frac{\psi_j}{\partial z}+C_{66}\frac{\partial\psi_i}{\partial z}\frac{\partial\psi_j}{\partial r}\right\}rdrdz\\
k_{21}&=\int\left\{C_{66}\frac{\partial\psi_i}{\partial r}\frac{\partial\psi_j}{\partial z}+C_{12}\frac{\partial\psi_i}{\partial z}\frac{\psi_j}{r}+C_{12}\frac{\partial\psi_i}{\partial z}\frac{\psi_j}{\partial r}-\frac{C_{66}}{r}\frac{\partial\psi_j}{\partial z}\psi_i\right\}rdrdz\\
k_{22}&=\int\left\{C_{66}\frac{\partial\psi_i}{\partial r}\frac{\partial\psi_j}{\partial r}+C_{11}\frac{\partial\psi_i}{\partial z}\frac{\psi_j}{\partial z}-\frac{C_{66}}{r}\frac{\partial\psi_j}{\partial r}\psi_i\right\}rdrdz\\
F_1&=\oint\psi_i t_r\,ds\\
F_2&=\oint\psi_i t_z\,ds
\end{aligned} \tag{14}$$

In Eqs. (14) integration is done over each element domain. To solve the problem in time domain, Newmark's method is used.

4 RESULTS AND DISCUSSION

The functionally graded cylinder is assumed to be made of a combination of metal (Ti–6Al–4V) and ceramic (ZrO_2), with the material properties shown in Table 1. The cylinder is ceramic-rich in the inner and metal-rich at the outer surfaces, respectively. Boundary conditions at two ends of the cylinder are considered free.

Metal: Ti–6Al–4V	Ceramic: ZrO_2
$\nu = 0.321$	$\nu = 0.333$
$E = 66.2$ (GPa)	$E = 117.0$ (GPa)
$\rho = 4.41\times10^3$ (kg/m^3)	$\rho = 5.6\times10^3$ (kg/m^3)

Table 1: Material properties of Titanium and Zirconia

To illustrate the results in thick cylinder and cylindrical shell, two ratios of inner radius to thickness are considered. These ratios are 1 for thick cylinder and 20 for cylindrical shell. For both type of cylinders, the ratio of length to inner radius is considered equal to 20. We consider volume fraction coefficient $n = 2$ as a sample of functionally graded cylinder.

4.1 Exponentially loading

Consider the internal pressure loading function as:

$$F(t) = P_0(1-e^{c_0 t}) \tag{15}$$

where p_0 and c_0 are constants and and assumed as p_0 =1 MPa and c_0 =100. For validation, Figure 2 shows the radial displacement along radial direction for long time in middle length of metal-rich thick cylinder. In this diagram the result of the above procedure is compared to the analytical result of an isotropic thick hollow cylinder under uniform internal pressure. A good agreement between these two results is observed.

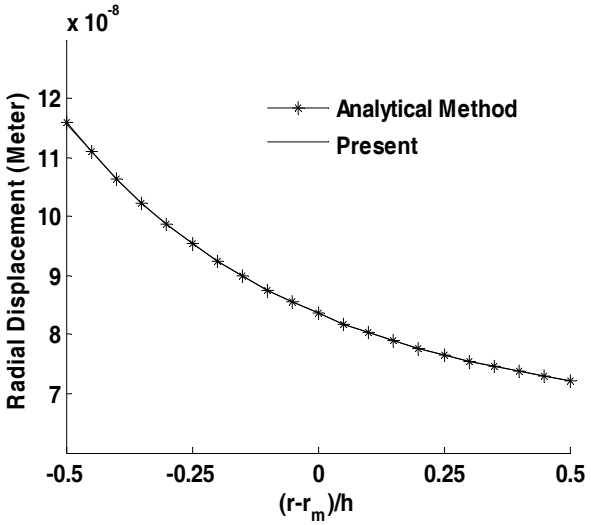

Figure 2: Radial displacement along radial direction of metal-rich cylinder for long time.

For $\Delta t = 0.1\,\mathrm{s}$, $F(t)$ approximately equals to final value. Radial displacement along radial direction at the middle length of functionally graded thick cylinder for different times in the interval Δt is illustrated in Figure 3. Similar diagram for functionally graded cylindrical shell is shown in Figure 4.

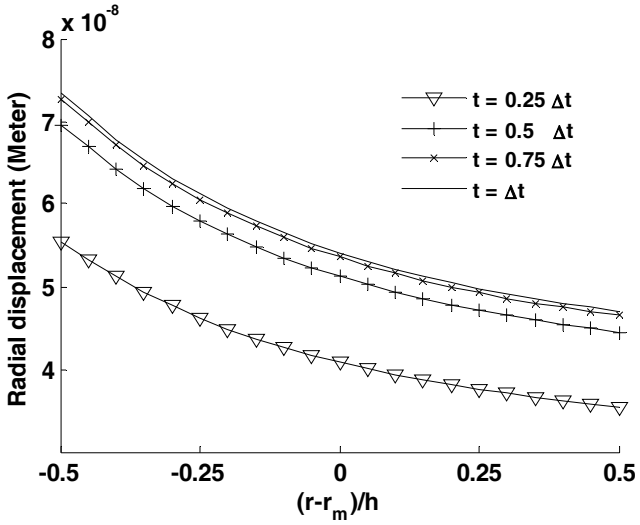

Figure 3: Transient radial displacement for thick cylinder.

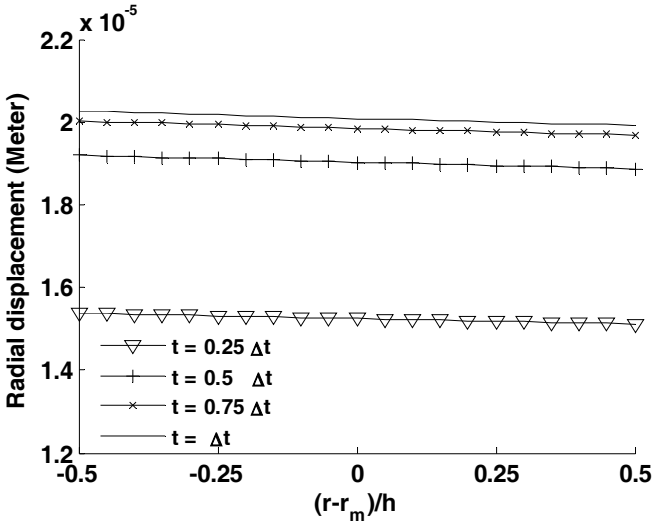

Figure 4: Transient radial displacement for cylindrical shell.

Comparing Figure 3 and Figure 4 shows that variation of radial displacement along radial direction for thick cylinder is greater than cylindrical shell.

4.2 Triangle pulse load

Consider the internal pressure applied as a triangle pulse load:

$$\begin{aligned} F(t) &= p_0 t \quad \text{for} \quad t \le t_0 \\ F(t) &= 0 \quad\;\; \text{for} \quad t > t_0 \end{aligned} \tag{16}$$

It is assumed that for thick cylinder p_0 =20 MPa and $t_0 = 0.5\times10^{-4}\,\mathrm{s}$ and for cylindrical shell p_0 =1 MPa and t_0 =0.001s. Time history of radial displacement of functionally graded and

pure thick cylinders are compared in Figure 5. Similar diagram for cylindrical shell is shown in Figure 6. These results are obtained for a point in the middle length and the middle thickness of cylinder.

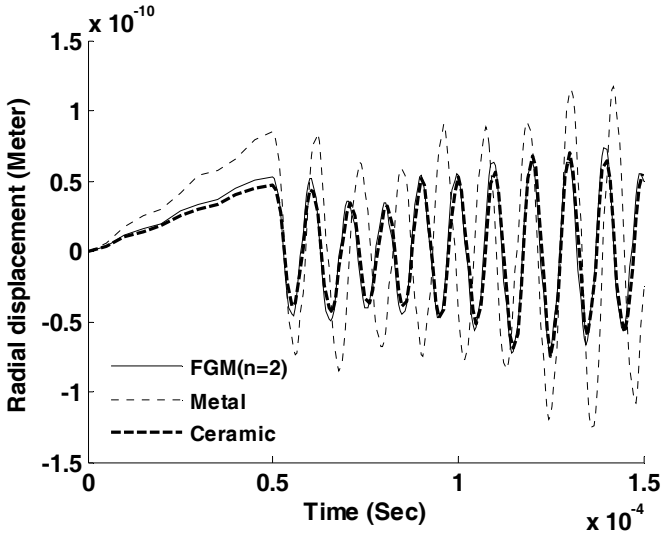

Figure 5: Time history of radial displacement in thick cylinder which is excited by triangle pulse load.

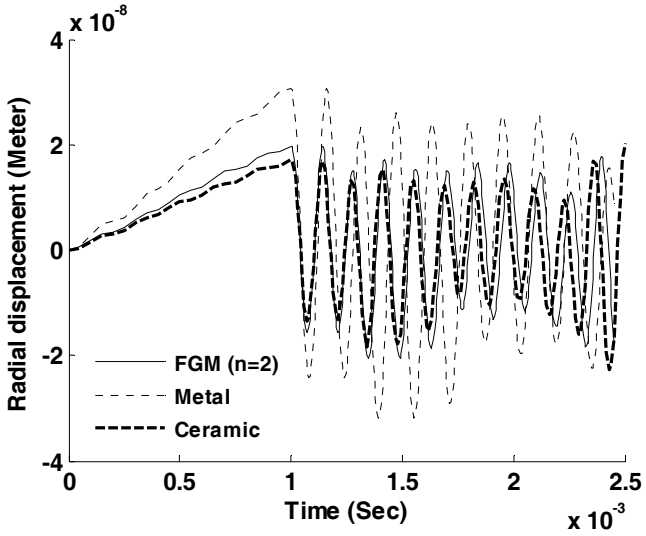

Figure 6: Time history of radial displacement in cylindrical shell which is excited by triangle pulse load.

From Figures 5 and 6 it is observed that the scope of the response due to the triangle pulse load for metal-rich cylinder is greater than ceramic-rich cylinder, because the module of elasticity for metal is less than ceramic. Also, the response of functionally graded cylinder is placed between the responses of metal-rich and ceramic-rich cylinders.

	Metal	FGM (n=2)	Ceramic
Thick cylinder	9045.2	10050.2	10101.0
Cylindrical shell	6228.4	6920.4	7382.6

Table 2: Natural frequencies of the cylinders.

By using the fast Fourier transform (FFT), the time response is transferred to frequency domain and natural frequencies are obtained as shown in Table 2. It is observed that the natural frequency for metal-rich cylinder is less than ceramic-rich cylinder and for thick cylinder is greater than cylindrical shell. Also, the natural frequency of functionally graded cylinder is between the natural frequencies of metal-rich and ceramic-rich cylinders.

Time history of radial stress for functionally graded and pure thick cylinders is shown in Figure 7. Similar results for cylindrical shell is shown in Figure 8.

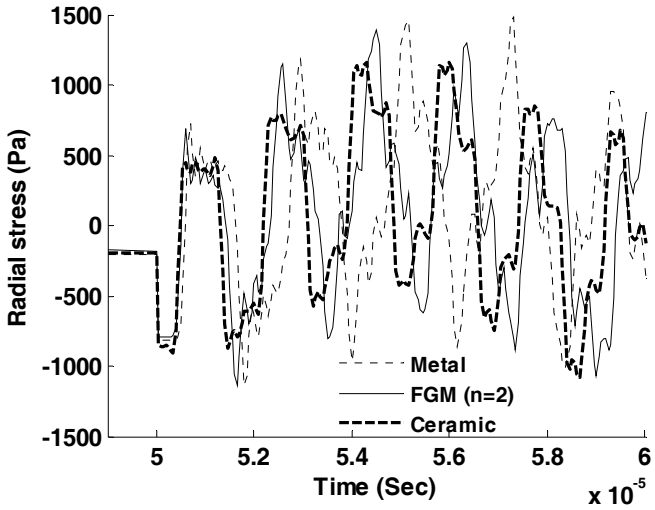

Figure 7: Time history of radial stress in thick cylinder which is excited by triangle pulse load.

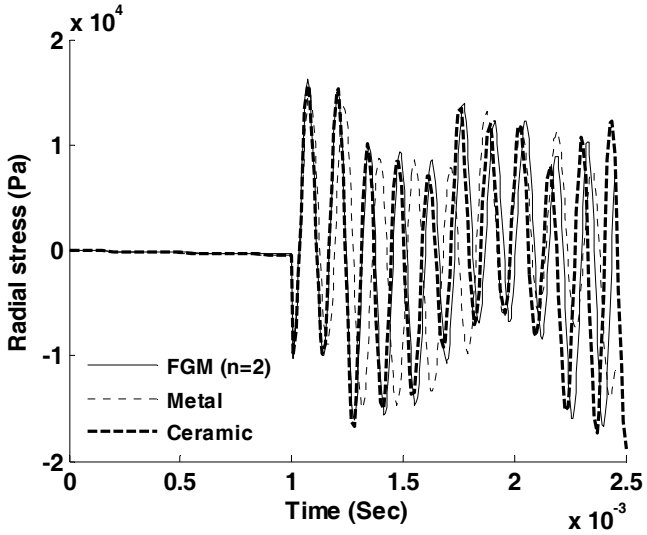

Figure 8: Time history of radial stress in cylindrical shell which is excited by triangle pulse load.

Also, time history of hoop stress for functionally graded and pure thick cylinders is shown in Figure 9. Similar results for cylindrical shell is shown in Figure 10.

4.3 Longitudinal wave propagation

Consider radial line load of $q = q_0 \delta(z) f(t)$ which is uniformly distributed along circumferential direction, where q_0=1 kN, and δ is Dirac delta function and $f(t)$ is an incident wavelet as:

$$\begin{aligned} f(t) &= \sin(2\pi t/\tau) \quad \text{for} \quad t \le \tau/4 \\ f(t) &= 0 \qquad\qquad\quad \text{for} \quad t > \tau/4 \end{aligned} \tag{17}$$

It is assumed that for thick cylinder $\tau = 2\pi \times 10^{-5}$ s and for cylindrical shell $\tau = 16\pi \times 10^{-5}$ s. The load is applied at one end of the cylinder and its effects on the middle length of cylinder are studied. Time history of radial displacement of functionally graded and pure thick cylinders is compared in Figure 11. Similar results for cylindrical shell is also shown in Figure 12.

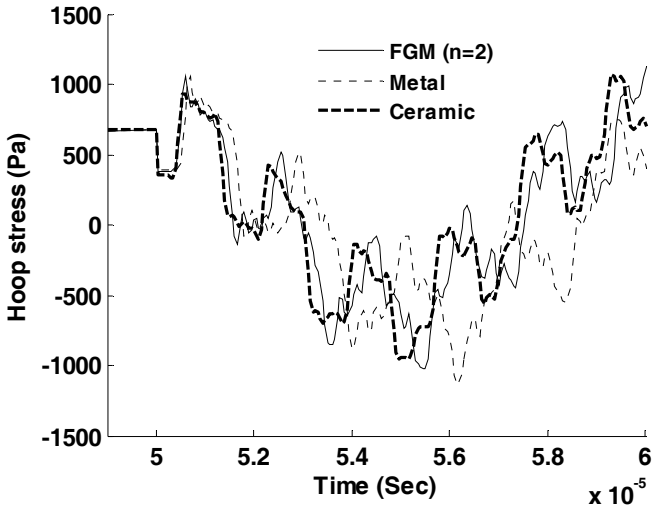

Figure 9: Time history of hoop stress in thick cylinder which is excited by triangle pulse load.

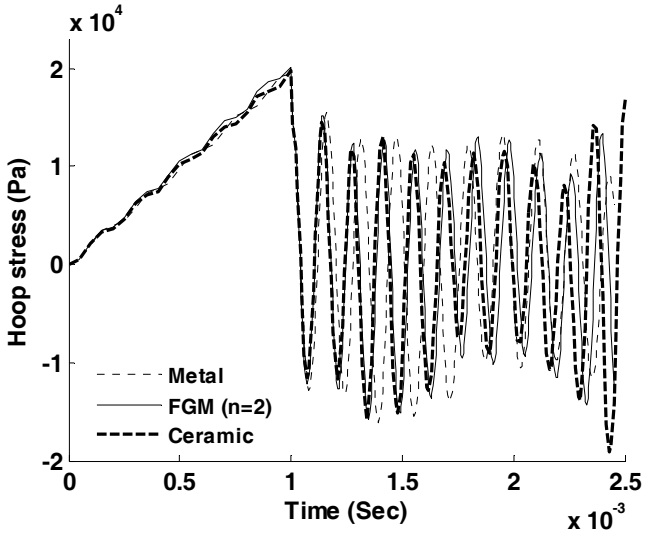

Figure 10: Time history of hoop stress in cylindrical shell which is excited by triangle pulse load.

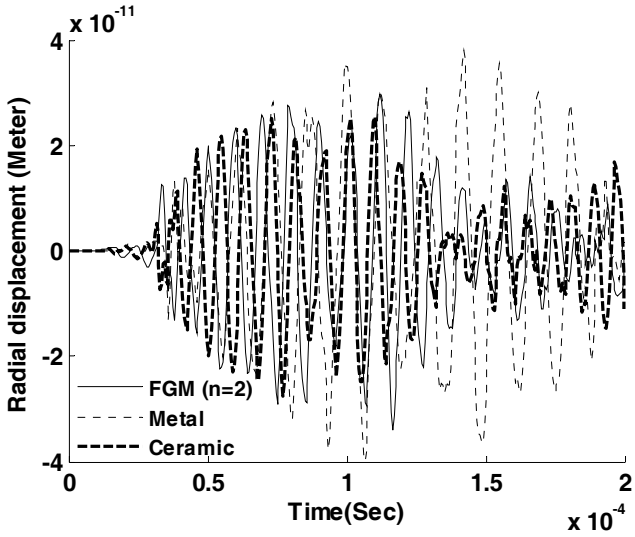

Figure 11: Time history of radial displacement in thick cylinder which is excited by incident wavelet.

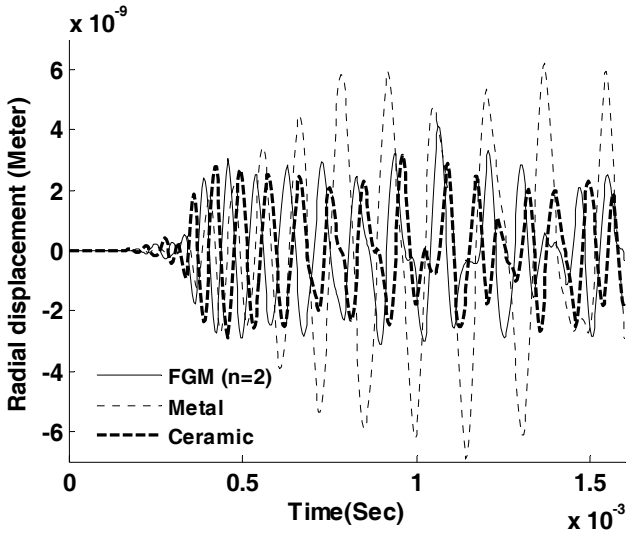

Figure 12: Time history of radial displacement in cylindrical shell which is excited by incident wavelet.

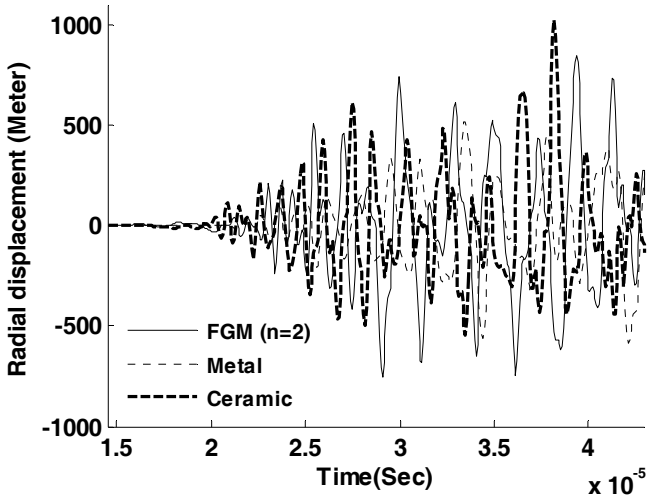

Figure 13: Time history of radial stress in thick cylinder which is excited by incident wavelet.

From displacement figures, it is observed that the response of functionally graded cylinder due to the incident wavelet is placed between the responses of metal-rich and ceramic-rich cylinders.

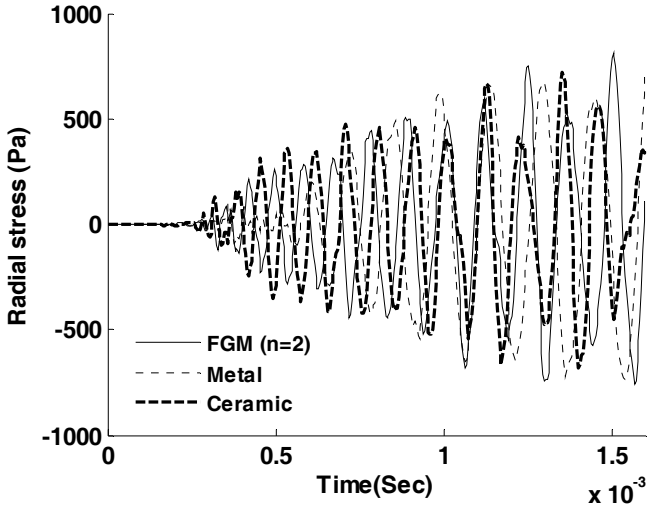

Figure 14: Time history of radial stress in cylindrical shell which is excited by incident wavelet.

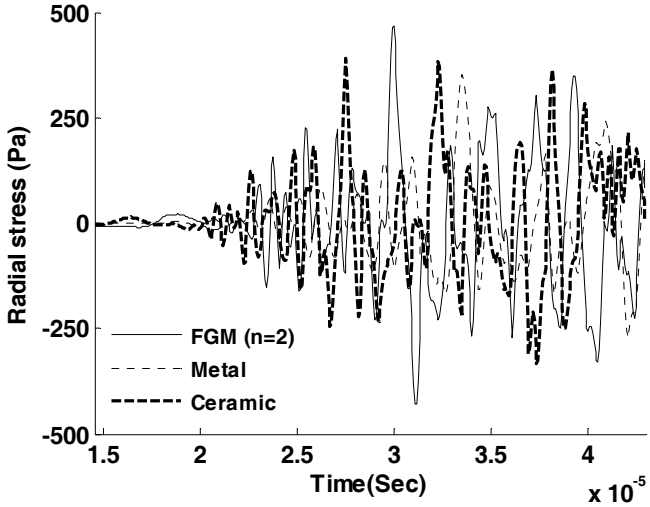

Figure 15: Time history of hoop stress in thick cylinder which is excited by incident wavelet.

From time history of displacement diagrams, the mean velocities of longitudinal wave propagation are obtained and shown in Table 3. It is observed that the mean velocity of longitudinal wave propagation for metal-rich cylinder is less than ceramic-rich cylinder and for cylindrical shell is greater than thick cylinder. Also, the mean velocity of longitudinal wave propagation for functionally graded cylinder is between the mean velocities of longitudinal wave propagation for metal-rich and ceramic-rich cylinders.

	Metal	FGM (n=2)	Ceramic
Thick cylinder	2222.2	2863.0	3218.4
Cylindrical shell	3888.8	5045.0	5656.6

Table 3: Mean velocities of longitudinal wave propagation.

Time history of radial stress for functionally graded and pure thick cylinders is shown in Figure 13. Similar results for cylindrical shell is shown in Figure 14. Also, time history of hoop stress for functionally graded and pure thick cylinders is shown in Figure 15. Similar results for cylindrical shell is shown in Figure 16.

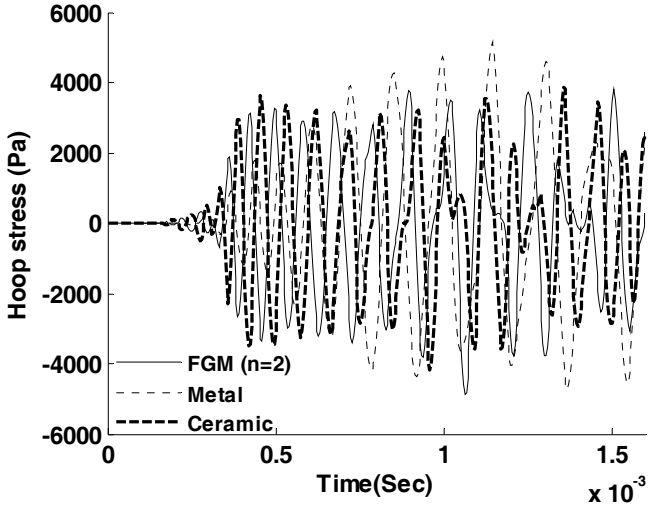

Figure 16: Time history of hoop stress in cylindrical shell which is excited by incident wavelet.

5 CONCLUSIONS

Analysis of functionally graded hollow cylinders with finite length under axisymmetric dynamic loads is presented. Two dimensional finite element and Newmark's methods are used to solve the governing equations of motion. Three types of dynamic loads are applied and the results are compared for thick and thin cylinders. Numerical results reveal that the scope of the displacement for metal-rich cylinder is greater than ceramic-rich cylinder while natural frequencies and wave velocity are less. These parameters for functionally graded cylinder are between the results of metal-rich and ceramic-rich cylinders.

REFERENCES

[1] S.W. Gong, K.Y. Lam, J.N. Reddy, *The elastic response of functionally graded cylindrical shells to low-velocity impact*, International Journal of Impact Engineering, 22, 397–417, 1999.

[2] R.B. Nelson, S.B. Dong, Kalrav RD, *Vibrations and waves in laminated orthotropic circular cylinders*, Journal of Sound and Vibration, 18(3), 429–44, 1971.

[3] X. Han, G.R. Liu, Z.C. Xi, K.Y. Lam, *Characteristics of waves in a functionally graded cylinder*, International Journal for Numerical Methods in Engineering, 53, 653–76, 2002.

[4] X. Han, G.R. Liu, Z.C. Xi, K.Y. Lam, *Transient waves in a functionally graded cylinder*, International Journal of Solids and Structures, 38, 3021–3037, 2001.

[5] X. Han, D. Xu, G.R. Liu, *Transient responses in a functionally graded cylindrical shell to a point load*, Journal of Sound and Vibration, 251, 783–805, 2002.

[6] C.T. Loy, K.Y. Lam, J.N. Reddy, *Vibration of functionally graded cylindrical shells*, International Journal of Mechanical Sciences, 41, 309–324, 1999.

[7] S.C. Pradhan, C.T. Loy, K.Y. Lam, J.N. Reddy, *Vibration characteristics of functionally graded cylindrical shells under various boundary conditions*, Applied Acoustics, 29, 61–111, 2000.

[8] J. Yang, H.S. Shen, *Free vibration and parametric resonance of shear deformable functionally graded cylindrical panels*, Journal of Sound and Vibration, 261, 871–893, 2003.

[9] J. Yang, H.S. Shen, *Parametric resonance of shear deformable functionally graded cylindrical panels in thermal environment*, Journal of Sound and Vibration, 261, 871–893, 2003.

[10] A.H. Sofiyev, *The stability of compositionally graded ceramic-metal cylindrical shells under aperiodic axial impulsive loading*, Composite Structures, 69, 247–257, 2005.

[11] A.H. Sofiyev, *Dynamic buckling of functionally graded cylindrical shells under non-periodic impulsive loading*, Acta Mechanica, 165, 153–62, 2003.

[12] A.H. Sofiyev, *The stability of functionally graded truncated conical shells subjected to aperiodic impulsive loading*, International Journal of Solids and Structures, 41, 3411–24, 2004.

[13] L. Elmaimouni, J.E. Lefebvre, V. Zhang, T. Gryba, *Guided waves in radially graded cylinders: a polynomial approach*, NDT&E International, 38, 344–353, 2005.

[14] R. Kadoli, N. Ganesan, *Buckling and free vibration analysis of functionally graded cylindrical shells subjected to a temperature specified boundary condition*, Journal of Sound and Vibration, 289, 450–480, 2006.

[15] M. Shakeri, M. Akhlaghi, S.M. Hoseini, *Vibration and radial wave propagation velocity in functionally graded thick hollow cylinder*, Composite Structures, 76, 174–184, 2006.

[16] T.Y. Ng, K.M. Lam, K.M. Liew, J.N. Reddy, *Dynamic stability analysis of functionally graded cylindrical shells under periodic axial loading*, International Journal of Solids and Structures, 38, 1295–1309, 2001.

[17] T.Y. Ng, X.Q. He, K.M. Liew, *Finite element modeling of active control of functionally graded shells in frequency domain via piezoelectric sensors and actuators*, Computational Mechanics, 28, 1–9, 2002.

[18] T. Fuchiyama, N. Noda, *Analysis of thermal stress in a plate of functionally gradient material*, JSAE Review, 16, 263–268, 1995.

[19] J.N. Reddy, C.D. Chin, *Thermomechanical analysis of functionally graded cylinders and plates*, Journal of Thermal Stresses, 21, 593–626, 1998.

[20] H. Awaji, R. Sivakumar, *Temperature and stress distribution in a hollow cylinder of functionally graded material: the case of temperature-independent material properties*, Journal of the American Ceramic Society, 84, 1059–1065, 2001.

[21] M.R. Eslami, R. Shahsiah, *Thermal buckling of imperfect cylindrical shells*, Journal of Thermal Stresses, 24, 1177–98, 2001.

[22] Y. Obata, K. Kanayama, T. Ohji, N. Noda, *Two-dimensional unsteady thermal stresses in a partially heated circular cylinder made of functionally graded material*, Proc Therm Stress ’99, Cracow, June, 595, 13–17, 1999.